Journal of Macromolecular Science, Part A
Publication details, including instructions for authors and subscription information:
http://www.informaworld.com/smpp/title~content=t713597274

A Comparison of Reaction Mechanisms for Reversible Addition-Fragmentation Chain Transfer Polymerization Using Modeling Tools

Jhonatan Pallares[a]; Gabriel Jaramillo-Soto[a]; Citlalli Flores-Cataño[a]; Eduardo Vivaldo Lima[ab]; Liliane M. F. Lona[c]; Alexander Penlidis[b]
[a] Departamento de Ingeniería Química, Facultad de Química, Universidad Nacional Autónoma de México (UNAM), Conjunto E, Ciudad Universitaria, México D. F., México [b] Institute for Polymer Research, Department of Chemical Engineering, University of Waterloo, Waterloo, Ontario, Canada [c] Departamento de Processos Químicos, Faculdade de Engenharia Química, Universidade Estadual de Campinas, Campinas, São Paulo, Brazil

To cite this Article Pallares, Jhonatan , Jaramillo-Soto, Gabriel , Flores-Cataño, Citlalli , Lima, Eduardo Vivaldo , Lona, Liliane M. F. and Penlidis, Alexander(2006) 'A Comparison of Reaction Mechanisms for Reversible Addition-Fragmentation Chain Transfer Polymerization Using Modeling Tools', Journal of Macromolecular Science, Part A, 43: 9, 1293 — 1322
To link to this Article: DOI: 10.1080/10601320600814614
URL: http://dx.doi.org/10.1080/10601320600814614

Journal of Macromolecular Science®, Part A: Pure and Applied Chemistry, 43:1293–1322, 2006

ISSN 1060-1325 print/1520-5738 online
DOI: 10.1080/10601320600814614

A Comparison of Reaction Mechanisms for Reversible Addition-Fragmentation Chain Transfer Polymerization Using Modeling Tools

JHONATAN PALLARES,[1] GABRIEL JARAMILLO-SOTO,[1] CITLALLI FLORES-CATAÑO,[1] EDUARDO VIVALDO LIMA,[1,2,‡] LILIANE M. F. LONA,[3] AND ALEXANDER PENLIDIS[2]

[1]Departamento de Ingeniería Química, Facultad de Química, Universidad Nacional Autónoma de México (UNAM), Conjunto E, Ciudad Universitaria, México D. F., México
[2]Institute for Polymer Research, Department of Chemical Engineering, University of Waterloo, Waterloo, Ontario, Canada
[3]Departamento de Processos Químicos, Faculdade de Engenharia Química, Universidade Estadual de Campinas, Campinas, São Paulo, Brazil

A kinetic model based on a detailed reaction mechanism of the reversible addition-fragmentation transfer (RAFT) polymerization was developed. By neglecting some reactions, or using simplifying assumptions, three different reaction mechanisms proposed in the literature can be described with this model. The resulting equations were solved using a self-developed Fortran code. The cases were also modeled using the Predici® commercial software. Parameter sensitivity analyses and a comparison of performance of the models for the different reaction mechanisms are presented. It was found that the simplest reaction mechanisms considered in this paper cannot adequately describe the behavior of the RAFT polymerization process. It is demonstrated that the controversy in the literature regarding the "six orders of magnitude difference" in the fragmentation rate coefficient, and the "concern" about the "validity" of the commercial software package Predici® to represent the RAFT mechanism have nothing to do with model inadequacy or the alluded "empirical nature" of Predici®. Rather, these issues are merely a matter of not having precise parameter estimates in a very complex, multi-parameter model, where similar model profiles can be generated with different combinations of model parameters.

Keywords controlled/living radical polymerization (CLRP), reversible addition fragmentation transfer (RAFT) polymerization, modeling, polymerization kinetics

Received and Accepted April 2006.
‡On research leave from UNAM.
Address correspondence to Eduardo Vivaldo Lima, Departamento de Ingeniería Química, Facultad de Química, Universidad Nacional Autónoma de México (UNAM), Conjunto E, Ciudad Universitaria, CP 04510, México D. F., México. Tel: +(5255)5622-5256; Fax: +(5255)5622-5355; E-mail: vivaldo@servidor.unam.mx

Introduction

Controlled/living radical polymerization (CLRP) is one of the most rapidly developing areas of polymer science. The ability to prepare well-defined block and graft copolymers, gradient and periodic copolymers, stars, combs, polymer networks, and end-functional polymers by free-radical mechanisms is perhaps the main reason for the increased academic and industrial interest in CLRP. The industrial interest is triggered by the potential of CLRP in areas such as coatings, adhesives, surfactants, dispersants, lubricants, gels, additives, thermoplastic elastomers as well as many electronic and biomedical applications (1).

RAFT polymerization (radical polymerization with reversible addition-fragmentation chain transfer) is arguably one of the most recent and effective methods in the CLRP field. Some of the advantages of RAFT polymerization over competing technologies (atom transfer radical polymerization, ATRP, and nitroxide-mediated radical polymerization, NMRP) stem from the fact that it is tolerant of a very wide range of functionality in monomer and solvent. This means that it is applicable to a large range of monomer types and that polymerizations and copolymerizations can be successfully carried out under a wide range of reaction conditions (bulk, solution, emulsion, suspension) (2).

Although the RAFT process is extremely versatile, it is important to recognize that not all of the RAFT agents work equally well in all circumstances, and that most of the RAFT controllers are not commercially available as of yet. Several reviews on CLRP and RAFT have been written. A recent one on the chemistry of RAFT polymerization was presented by Moad et al. (3).

In the case of RAFT processes, Li et al. (4) modeled the kinetics and molecular weight development using the Monte Carlo technique. Zhang and Ray (5) developed a comprehensive kinetic model for polymerization kinetics and calculation of molecular weight averages using the method of moments. Barner-Kowollik et al. (6) used the Predici® commercial package to simulate the polymerization kinetics and molecular weight development. Wang and Zhu (7) also used the method of moments, based on a simplified reaction mechanism (suppressing the reversibility in the addition-fragmentation reactions), to model the evolution of the molecular weight averages. They also considered diffusion-controlled effects in the reactions involving macromolecules (not only diffusion-controlled termination) (8). Luo (9) used the Monte Carlo technique to model the initial stages of RAFT seeded emulsion polymerization. Drache et al. (10) also used the Monte Carlo simulation technique to model the polymerization kinetics of RAFT batch processes. Theis et al. (11) simulated the RAFT process considering chain-length dependent termination using the Predici® commercial package. Monteiro (12) modeled the molecular weight development (number average molecular weight, M_n, and polydispersity index, PDI) in block copolymer formation with the RAFT process. Finally, Peklak et al. (13) modeled the molecular weight development of the RAFT process by directly solving the population balance equations, instead of only calculating the moments of the molecular weight distribution (MWD), and considered free-volume dependence of the kinetic rate constants associated with reactions with macromolecules, to take into account diffusion-controlled effects on the polymerization kinetics and the MWD.

There is an ongoing controversial debate in the literature regarding the mechanism that causes rate retardation phenomena in some RAFT polymerization systems (see for instance the corresponding section of Reference 3). The analysis of this problem has created another debate about the magnitude of the fragmentation rate constant (k_b in our nomenclature) for some of these RAFT polymerization systems. Wang and Zhu (7)

used a value of $k_b = 10^4\ s^{-1}$ in the reference set of kinetic rate constants for their model simulations, and suggested in their conclusions that the radical adduct (the macroRAFT radical) was a very short-lived species. Barner-Kowollik et al. (14) criticized that statement from Wang and Zhu (7) and pointed out that there is experimental and theoretical evidence suggesting that the macroRAFT radical is a stable species with a lifetime longer than the 0.0001 s assumed by Wang and Zhu (7). They also pointed out that Wang and Zhu (7) used a very high value of the cross-termination kinetic rate constant, and that they provided a purely simulation study, with no experimental data. In replying to the comments from Barner-Kowollik et al. (14), Wang et el. (15) provided an explanation of how the kinetic rate constants were chosen, and addressed other related issues. However, in their reply paper, Wang et al. (15) criticized the "amended" scheme used by Barner-Kowollik et al. (6) to simulate the RAFT process with the Predici® software, stating that the concentration of the macroRAFT radicals could not be calculated with that scheme, and regarded the Predici® modeling of RAFT as semiempirical. Wulkow et al. (16) subsequently described the mathematical model behind the Predici® implementation from Barner-Kowollik et al. (6) of the RAFT process, and concluded that the implementation using two memory distribution species is a valid and quantitative translation of the original CSIRO-suggested RAFT mechanism (3, 17). Unfortunately, they did not provide calculations of the concentration profiles of the macroRAFT radicals, which was one of the aspects criticized by Wang et al. (15).

In this contribution, we present a comprehensive mathematical model for the RAFT process, based on a detailed reaction mechanism. Molecular weight development is calculated using the method of moments. The resulting mathematical model is similar to the one proposed by Zhang and Ray (5), but our model includes the possible termination reaction between macroRAFT radicals and living polymer radicals (18–21), and thermal self-initiation, both cases not considered by Zhang and Ray (5). Our model can easily reduce to simpler reaction mechanisms proposed by others, by adequate selection of the initial conditions and the values of some of the kinetic rate constants. Three different reaction mechanisms used in the literature are compared, and the validity of the predictions obtained with the Predici® commercial software is also addressed. The "typical" polymerization conditions used by Wang and Zhu (7) in their simulations and the RAFT polymerization of styrene using cumyl dithiobenzoate and 2,2-azobisisobutyronitrile (AIBN) at 60°C (6) were used as reference cases for our modeling study.

Experimental

Although the focus of this paper is on modeling of the RAFT process, one of the reference cases used to test our model is the system studied experimentally by Barner-Kowollik et al. (6). As mentioned before, this system consisted of the polymerization of styrene using cumyl dithiobenzoate as RAFT agent and 2,2-azobisisobutyronitrile (AIBN) as initiator, at 60°C.

Modeling

Reaction Mechanism

The detailed reaction mechanism used to derive our kinetic model is shown in Table 1. All the symbols used in the reactions of Table 1 and in our model equations that follow are defined in the nomenclature section. The CSIRO mechanism of RAFT polymerization

Table 1
Reaction mechanism for the "complete model" (Model 1)

Reaction #	Reaction name	Reaction step(s)
1	Chemical initiation	$I \xrightarrow{k_d} 2R_{in}^{\bullet}$ $R_{in}^{\bullet} + M \xrightarrow{k_i} RM_1^{\bullet}$
2	Thermal self-initiation	$M + M \xrightarrow{k_{dim}} D$ $D + M \xrightarrow{k_{thi}} D^{\bullet} + M^{\bullet}$
3	Propagation	$RM_r^{\bullet} + M \xrightarrow{k_p} RM_{r+1}^{\bullet}$
4	Chain transfer to monomer	$RM_r^{\bullet} + M \xrightarrow{k_{fm}} RD_r + M^{\bullet}$
5	Chain transfer to solvent	$RM_r^{\bullet} + S \xrightarrow{k_{fS}} RD_r + S^{\bullet}$
6	Chain transfer to chain transfer agent (CTA)	$RM_r^{\bullet} + CTA \xrightarrow{k_{fT}} RD_r + CTA^{\bullet}$
7	Irreversible chain transfer to RAFT Agent	$RM_r^{\bullet} + AB \xrightarrow{k_{tr}} RM_rA + B^{\bullet}$
8	Reversible chain transfer to RAFT Agent	$RM_r^{\bullet} + AB \underset{k_{-add}}{\overset{k_{add}}{\rightleftarrows}} RM_r\dot{A}B \underset{k_{-bd}}{\overset{k_{bd}}{\rightleftarrows}} RM_rA + B^{\bullet}$
9	Reinitiation	$B^{\bullet} + M \xrightarrow{k_i} BM_1^{\bullet}$ $M^{\bullet} + M \xrightarrow{k_i} MM_1^{\bullet}$ $D^{\bullet} + M \xrightarrow{k_i} DM_1^{\bullet}$ $S^{\bullet} + M \xrightarrow{k_i} SM_1^{\bullet}$ $CTA^{\bullet} + M \xrightarrow{k_i} CTAM_1^{\bullet}$ $\Big\} RM_1^{\bullet}$
10	Chain equilibration (addition-fragmentation)	$RM_r^{\bullet} + RM_sA \underset{k_{-a}}{\overset{k_a}{\rightleftarrows}} RM_r\dot{A}RM_s \underset{k_{-b}}{\overset{k_b}{\rightleftarrows}} RM_rA + RM_s^{\bullet}$
11	Termination by disproportionation	$RM_r^{\bullet} + RM_s^{\bullet} \xrightarrow{k_{td}} RD_r + RD_s$
12	Termination by combination	$RM_r^{\bullet} + RM_s^{\bullet} \xrightarrow{k_{tc}} RD_{r+s}R$
13	Intermediate radical termination	$RM_p\dot{A}RM_q + RM_r^{\bullet} \xrightarrow{k_{tir}} RM_pRM_qRM_r$

includes the reactions of chemical initiation (#1 in Table 1), reversible chain transfer (#8 in Table 1), reinitiation of the RAFT segment (the first of the 5 reactions shown in row #9 of Table 1), chain equilibration (#10 in Table 1), and bimolecular termination (#11 and #12 in Table 1) (2, 3, 17). In addition to the original reactions considered in the RAFT

process, we have included the possibility of thermal self-initiation (#2 in Table 1) (22, 23), given that successful RAFT polymerizations have been performed over the range 20–150°C (2), as well as transfer to monomer, solvent and added non-RAFT chain transfer agents (# 4,5 and 6 of Table 1) (5). The formation of a three armed star from the reaction between a polymeric adduct or macroRAFT radical (species $RM_rA^{\bullet}RM_s$ in Table 1) and a growing free radical (18–21) (#13 in Table 1) was also considered in the reaction mechanism. The possibility of the transfer to RAFT agent reaction proceeding irreversibly (6, 24) is considered by using reaction #7 instead of reaction #8 of Table 1. The kinetic model derived from the reaction mechanism shown in Table 1 will be referred to as the "complete model", or "Model 1".

The kinetic model developed by Wang and Zhu (7, 8) is based on a reaction mechanism consisting of reactions 1, 3, 11, 12 and 13 of Table 1. Regarding the addition-fragmentation reactions with RAFT chain transfer agent and dormant polymer molecules, instead of reactions 7–8 and 10 of Table 1, they used a single reaction, shown below in equation (1). It should be noted that Wang and Zhu (7, 8) assumed the individual addition and fragmentation reactions to be irreversible, and that the addition of polymer radicals with a RAFT controller and the fragmentation of the formed adduct proceed with the same rates as the corresponding addition-fragmentation reactions with dormant polymer molecules. The kinetic model based on reaction #1, 3, 11–13 of Table 1, and on the reaction shown below as equation (1), namely the Wang-Zhu model (7, 8), will be referred to as the "irreversible model" or "Model 2".

$$RM_r^{\bullet} + RM_sA \xrightarrow{k_a} RM_r\dot{A}RM_s \xrightarrow{k_b} RM_rA + RM_s^{\bullet} \tag{1}$$

The possibility of the reversible chain transfer to RAFT agent and chain equilibration reactions (reaction #8 and 10 in Table 1, respectively) proceeding with very short lifetimes of the corresponding intermediate adducts (i.e., the reversible chain transfer between living and dormant (or RAFT transfer agent) species without the direct presence in the reaction mechanism of the intermediate adducts (24)), given by the reactions shown below in Equations (2) and (3), was also considered. The third case, based on the reaction mechanism given by #1–7, 9, 11–13 of Table 1, and Equations (2) and (3) below, will be referred to as the "simplified model", or "Model 3". The relationship of rate constants k_1, k_2, k_3 and k_4 with the addition/fragmentation constants of #8 and 10 of Table 1 will be explained later, in the results and discussion section of this paper.

$$RM_r^{\bullet} + AB \underset{k_2}{\overset{k_1}{\rightleftharpoons}} RM_rA + B^{\bullet} \tag{2}$$

$$RM_r^{\bullet} + RM_sA \underset{k_4}{\overset{k_3}{\rightleftharpoons}} RM_rA + RM_s^{\bullet} \tag{3}$$

Model Equations

Mass Balance Equations for Small Molecules. Based on the reaction mechanism shown in Table 1, the mass balance equations for a batch reactor are given by Equations (4) to (15), for small molecules. The moments of the polymer distributions are defined in Table 2. The rates of initiator decomposition, monomer, dimer, solvent and non-RAFT chain transfer

Table 2
Definition of moments of the polymer distributions

Species	Definition of moments
Polymer radicals (living polymer)	$Y_m = \sum_{r=1}^{\infty} r^m [RM_r^\bullet]$
Dormant polymer	$Z_m = \sum_{r=1}^{\infty} r^m [RM_r A]$
Dead polymer from termination by disproportionation and transfer to small molecules	$Q_m = \sum_{r=1}^{\infty} r^m [RD_r]$
Dead polymer from termination by combination	$S_m = \sum_{r=1}^{\infty} r^m [RD_r R]$
One arm adduct	$E_m = \sum_{r=1}^{\infty} r^m [RM_r A^\bullet B]$
Two arms adduct (macroRAFT radical)	$F_{mn} = \sum_{r=1}^{\infty} \sum_{s=1}^{\infty} r^m s^n [RM_r A^\bullet RM_s]$
Three arms dead polymer	$G_{abc} = \sum_{p=1}^{\infty} \sum_{q=1}^{\infty} \sum_{r=1}^{\infty} p^a q^b r^c [RM_p RM_q RM_r]$

agent (CTA) consumption are given by Equations (4) to (8). Equations (9) to (13) are the corresponding rate equations for primary, monomeric, dimeric, and free radicals from chain transfer to solvent and CTA, respectively. Equation (14) shows the rate of consumption of the RAFT transfer agent. Both irreversible and reversible chain transfer to RAFT agent (reaction # 7 and 8, respectively, in Table 1) have been grouped in the same equation. If the reaction is irreversible, then the kinetic rate constants k_{add}, k_{-add}, k_{bd} and k_{-bd} take all the value of zero. If the reaction is reversible, then k_{tr} is set equal to zero. The same holds for Equation (15), which represents the rate of change of the concentration of primary radicals from the RAFT transfer agent (the R group in the representation of a RAFT transfer agent molecule, shown in Figure 1, once detached from the molecule).

$$\frac{d(V[I])}{Vdt} = -k_d[I] \tag{4}$$

$$\frac{d(V[M])}{Vdt} = -k_i[M]([R_{in}^\bullet] + [B^\bullet] + [M^\bullet] + [D^\bullet] + [S^\bullet] + [CTA^\bullet]) - k_{dim}[M]^2 - k_{thi}[M][D] - k_p[M][Y_0] - k_{fm}[M][Y_0] \tag{5}$$

$$\frac{d(V[D])}{Vdt} = k_{dim}[M]^2 - k_{thi}[M][D] \tag{6}$$

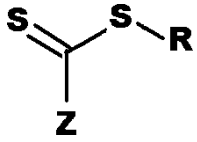

Figure 1. General chemical structure of a RAFT transfer agent. R is a free radical leaving group ($R^\bullet$ must be able to reinitiate polymerization). Substituent Z modifies the rates of addition and fragmentation. Examples of Z include aryl, alkyl (dithioesters), S-alkyl (trithiocarbonates), O-alkyl (xanthates), or N,N-dialkyl (dithiocarbamates) (3).

$$\frac{d(V[S])}{Vdt} = -k_{fS}[S][Y_0] \tag{7}$$

$$\frac{d(V[CTA])}{Vdt} = -k_{fT}[CTA][Y_0] \tag{8}$$

$$\frac{d(V[R_{in}^{\bullet}])}{Vdt} = 2fk_d[I] - k_i[R_{in}^{\bullet}][M] \tag{9}$$

$$\frac{d(V[M^{\bullet}])}{Vdt} = k_{thi}[M][D] + k_{fm}[M][Y_0] - k_i[M][M^{\bullet}] \tag{10}$$

$$\frac{d(V[D^{\bullet}])}{Vdt} = k_{thi}[D][M] - k_i[M][D^{\bullet}] \tag{11}$$

$$\frac{d(V[S^{\bullet}])}{Vdt} = k_{fS}[S][Y_0] - k_i[M][S^{\bullet}] \tag{12}$$

$$\frac{d(V[CTA^{\bullet}])}{Vdt} = k_{fT}[CTA][Y_0] - k_i[M][CTA^{\bullet}] \tag{13}$$

$$\frac{d(V[AB])}{Vdt} = -k_{tr}[AB][Y_0] - k_{add}[AB][Y_0] + k_{-add}[E_0] \tag{14}$$

$$\frac{d(V[B^{\bullet}])}{Vdt} = k_{tr}[AB][Y_0] + k_{bd}[E_0] - k_{-bd}[Z_0][B^{\bullet}] - k_i[M][B^{\bullet}] \tag{15}$$

If the simplified model (Model 3), represented by Equations (2) and (3) for the reactions with the RAFT transfer agent, is used, then Equations (14) and (15) should be replaced by Equations (16) and (17).

$$\frac{d(V[AB])}{Vdt} = -k_1[AB][Y_0] + k_2[B^{\bullet}][Z_0] \tag{16}$$

$$\frac{d(V[B^{\bullet}])}{Vdt} = k_1[AB][Y_0] - k_2[Z_0][B^{\bullet}] - k_i[M][B^{\bullet}] \tag{17}$$

Mass Balances for Polymeric Species

There are seven polymeric species considered in this work to participate in the RAFT process: linear polymer radicals (linear living or growing polymer), dormant polymer, dead polymer produced from termination by disproportionation, dead polymer produced from termination by combination, one-arm adduct (the product of the addition reaction between a living polymer molecule and a RAFT transfer agent), two-arm adduct (the product of the addition reaction between a living polymer molecule and a dormant polymer molecule), and three-arm dead polymer (the product from termination by combination between a living polymer molecule and a two-arm adduct). The corresponding mass balances for these seven polymeric species, based on the reaction mechanism of Table 1, are given by Equations (18) to (24). Caution must be exercised when using Equations (18) and (19) and the moment equations based upon them (see next section), since they contain the terms of Model 1 and Model 3 in the same equations. Depending

on the model being used (either model 1 or model 3), the kinetic rate constants should be appropriately (de)activated (e.g., $k_1 = k_2 = k_3 = k_4 = 0$ when model 1 is being used, or $k_{add} = k_{-add} = k_{bd} = k_{-bd} = k_a = k_b = k_{-b} = 0$ when model 3 is being used).

$$\begin{aligned}\frac{d(V[RM_r^\bullet])}{Vdt} &= 2fk_d[I] + k_i[M]([B^\bullet] + [M^\bullet] + [D^\bullet] + [S^\bullet] + [CTA^\bullet]) \\ &\quad + k_p[M]([RM_{r-1}^\bullet] - [RM_r^\bullet]) - [RM_r^\bullet](k_{fm}[M] + k_{fS}[S] \\ &\quad + k_{fT}[CTA] + k_{tr}[AB]) - (k_{td} + k_{tc})[RM_r^\bullet]\sum_{s=1}^{\infty}[RM_s^\bullet] - k_{tir}[RM_r^\bullet] \\ &\quad \times \sum_{p=1}^{\infty}\sum_{q=1}^{\infty}[RM_p\dot{A}RM_q] - k_1[AB][RM_r^\bullet] + k_2[B^\bullet][RM_rA] \\ &\quad - k_3[RM_r^\bullet]\sum_{S=1}^{\infty}[RM_sA] + k_4[RM_rA]\sum_{S=1}^{\infty}[RM_s^\bullet] - k_{add}[AB][RM_r^\bullet] \\ &\quad + k_{-add}[RM_r\dot{A}B] - k_a[RM_r^\bullet]\sum_{S=1}^{\infty}[RM_sA] + k_{-a}\sum_{s=1}^{\infty}[RM_r\dot{A}RM_s] \\ &\quad + k_b\sum_{s=1}^{\infty}[RM_r\dot{A}RM_s] - k_{-b}[RM_r^\bullet]\sum_{S=1}^{\infty}[RM_sA] \end{aligned} \tag{18}$$

$$\begin{aligned}\frac{d(V[RM_rA])}{Vdt} &= k_{tr}[AB][RM_r^\bullet] + k_1[AB][RM_r^\bullet] - k_2[RM_rA][B^\bullet] \\ &\quad + k_3[RM_r^\bullet]\sum_{s=1}^{\infty}[RM_sA] - k_4[RM_rA]\sum_{s=1}^{\infty}[RM_s^\bullet] \\ &\quad - k_a[RM_rA]\sum_{s=1}^{\infty}[RM_s^\bullet] + k_{-a}\sum_{s=1}^{\infty}[RM_r\dot{A}RM_s] \\ &\quad + k_b\sum_{s=1}^{\infty}[RM_r\dot{A}RM_s] - k_{-b}[RM_rA]\sum_{s=1}^{\infty}[RM_s^\bullet] \end{aligned} \tag{19}$$

$$\frac{d(V[RD_r])}{Vdt} = \left(k_{fm}[M] + k_{fS}[S] + k_{fT}[CTA] + k_{td}\sum_{s=1}^{\infty}RM_s^\bullet\right)[RM_r^\bullet] \tag{20}$$

$$\frac{d(V[RD_rR])}{Vdt} = \frac{k_{tc}}{2}\sum_{s=1}^{r-1}([RM_s^\bullet][RM_{r-s}^\bullet]) \tag{21}$$

$$\begin{aligned}\frac{d(V[RM_r\dot{A}B])}{Vdt} &= k_{add}[AB][RM_r^\bullet] - k_{-add}[RM_r\dot{A}B] \\ &\quad - k_{bd}[RM_r\dot{A}B] + k_{-bd}[B^\bullet][RM_rA] \end{aligned} \tag{22}$$

$$\begin{aligned}\frac{d(V[RM_r\dot{A}RM_s])}{Vdt} &= k_a[RM_r^\bullet][RM_sA] - k_{-a}[RM_r\dot{A}RM_s] \\ &\quad - k_b[RM_r\dot{A}RM_s] + k_{-b}[RM_s^\bullet][RM_rA] \end{aligned} \tag{23}$$

$$\frac{d(V[RM_pRM_qRM_r])}{Vdt} = k_{tir}[RM_p \dot{A} RM_q][RM_r^\bullet] \tag{24}$$

Moment Equations and Molecular Weight Averages

The moment equations needed to calculate averages of the molecular weight distribution are obtained upon application of the method of moments to equations (18) to (24), thus yielding Equations (25) to (32).

$$\begin{aligned}\frac{d(VY_m)}{Vdt} &= 2fk_d[I] + k_i[M]([B^\bullet] + [M^\bullet] + [D^\bullet] + [S^\bullet] + [CTA^\bullet]) + \beta_m \\ &\quad - (k_{fm}[M] + k_{fS}[S] + k_{fT}[CTA] + k_{tr}[AB])Y_m - (k_{td} + k_{tc})Y_0Y_m - k_{tir}Y_mF_{00} \\ &\quad - k_1[AB]Y_m + k_2[B^\bullet]Z_m - k_3Z_0Y_m + k_4Y_0Z_m - k_{add}[AB]Y_m \\ &\quad + k_{-add}E_m - k_aZ_0Y_m + k_{-a}F_{m0} + k_bF_{m0} - k_{-b}Z_0Y_m \end{aligned} \tag{25}$$

The term β_m used in Equation (25) is defined in Equation (26), and it depends on the value of m being evaluated. Equation (26) shows the cases for m = 0, 1 and 2, which are the only ones needed for calculation of M_n and M_w.

$$\beta_m = \begin{cases} 0, \text{ if } m = 0 \\ k_p[M]Y_0, \text{ if } m = 1 \\ k_p[M](Y_0 + 2Y_1), \text{ if } m = 2 \end{cases} \tag{26}$$

$$\begin{aligned}\frac{d(VZ_m)}{Vdt} &= k_{tr}[AB]Y_m + k_1[AB]Y_m - k_2[B^\bullet]Z_m + k_3Z_0Y_m \\ &\quad - k_4Y_0Z_m - k_aY_0Z_m + k_{-a}F_{m0} + k_bF_{m0} - k_{-b}Y_0Z_m \end{aligned} \tag{27}$$

$$\frac{d(VQ_m)}{Vdt} = (k_{fm}[M] + k_{fS}[S] + k_{fT}[CTA] + k_{td}Y_0)Y_m \tag{28}$$

$$\frac{d(VS_m)}{Vdt} = \frac{k_{tc}}{2}\sum_{n=1}^{m-1}\binom{m}{n}Y_nY_{m-n} \tag{29}$$

$$\frac{d(VE_m)}{Vdt} = k_{add}[AB]Y_m - k_{-add}E_m - k_{bd}E_m + k_{-bd}[B^\bullet]Z_m \tag{30}$$

$$\frac{d(VF_{mn})}{Vdt} = k_aY_mZ_n - k_{-a}F_{mn} - k_bF_{mn} + k_{-b}Z_mY_n \tag{31}$$

$$\frac{d(VG_{abc})}{Vdt} = k_{tir}F_{ab}Y_c \tag{32}$$

Number and weight average molecular weights, M_n and M_w, are calculated from the first three moments of the molecular weigh distributions of the different polymeric species that participate in the polymerization. The values of M_n and M_w for the overall polymer

population can be calculated using equations (33) and (34). The polydispersity index (PDI) is calculated using Equation (35).

$$M_n = \frac{Y_1 + Z_1 + Q_1 + S_1 + E_1 + F_{10} + F_{01} + G_{100} + G_{010} + G_{001}}{Y_0 + Z_0 + Q_0 + S_0 + E_0 + F_{00} + G_{000}} M_{rep} \quad (33)$$

$$M_w = \frac{\begin{array}{c} Y_2 + Z_2 + Q_2 + S_2 + E_2 + F_{20} + F_{02} + F_{11} + G_{200} \\ +G_{020} + G_{002} + G_{110} + G_{101} + G_{011} \end{array}}{Y_1 + Z_1 + Q_1 + S_1 + E_1 + F_{10} + F_{01} + G_{100} + G_{010} + G_{001}} M_{rep} \quad (34)$$

$$PDI = \frac{M_w}{M_n} \quad (35)$$

It is observed from Equations (33) and (34) that in order to calculate M_n and M_w, 7 order zero, 10 order one and 14 order two moments are needed. The 31 ordinary differential equations needed to calculate these moments can be easily generated from Equations (25) to (32) by just replacing the order of the moment (subscripts m, n, a, b or c in those equations) with 0, 1 or 2, as needed.

Numerical Issues and Implementation in Predici®

The complete model (Model 1) consists of 46 simultaneous ordinary differential equations (ODEs), 15 for small molecules (1–15), and 31 moment equations. The model equations were implemented in a Fortran computing program. Subroutine DDASSL (25) was used to numerically integrate the ODEs. The simulations presented in this study were generated using this code. Most of them were reproduced using the Predici® commercial software.

One problem with Predici® is that it does not include a direct reversible reaction between macromolecules in its database of reaction "steps". In order to implement reactions such as the addition and fragmentation reactions of RAFT, temporary chain size memory species have to be used (6, 16), although it has been shown that mathematically this approach is the same as having the direct reversible steps (16). It is important to mention that Predici® works by creating a reaction mechanism from a database of predefined reaction steps. Since some of these steps are similar, it is possible to create a single reaction mechanism in slightly different ways. In the end, the mathematical problem to be solved will be the same, provided that the reaction mechanism is implemented properly. Table 3 shows an example of implementing in Predici® (selection of "steps", reaction types and kinetic constants) a subset of model 1 of Table 1, for illustrative purposes.

Results and Discussion

The first system considered in this study (Case 1) was the "typical" RAFT formulation modeled by Wang and Zhu (7). The polymerization conditions and kinetic parameters used in our simulations are summarized in the caption of Figure 2. The selection of this system served the double purpose of testing the capability of our simulation program, based on the "complete model" (model 1) described earlier, to reproduce the results of Zhu and Wang (7), using what we call the "irreversible model" (Figures 2–4). The second purpose of choosing the "typical" formulation of Wang and Zhu (7) was to compare our simulations with the implementation in Predici® of that reaction mechanism, and using the same set of polymerization conditions and kinetic rate constants (Figures 2 and 4). The same RAFT polymerization system was used to compare the predictions of polymerization rate and molecular weight development

Table 3
Implementation of a subset of the "complete" RAFT mechanism in Predici®

Reaction # of Table 1	Step in Predici	Name of step	Kinetic rate constant (equivalent)
1	$I \rightarrow Rin^* + Rin^*$	Elementalreaction	k_d
1	$Rin^* + M \rightarrow RM^*(1)$	Initiation(n-mer)	k_i
9	$B^* + M \rightarrow RM^*(1)$	Initiation(n-mer)	k_i
3	$RM^*(s) + M \rightarrow RM^*(s+1)$	Propagation	k_p
8	$RM^*(s) + AB \rightarrow RMAB(s)$	Change	k_a
8	$RMAB(s) \rightarrow RMA(s) + B^*$	Change	k_b
10	$RM^*(s) + RMA(r) \rightarrow D(s) + DA(r)$	d-Termination	k_a
10	$D(s) \rightarrow RM^*(s)$	Change	k_b
10	$D(s) \rightarrow RMA(s)$	Change	k_b
10	$DA(s) \rightarrow RM^*(s)$	Change	k_b
10	$DA(s) \rightarrow RMA(s)$	Change	k_b
13	$D(s) + RM^*(r) \rightarrow T1(s) + T3(r)$	d-Termination	k_{tir}
13	$DA(s) + RM^*(r) \rightarrow T2(s) + T3(r)$	d-Termination	k_{tir}
13	$D(s) \rightarrow T1(s)$	Change	k_{tir}
13	$DA(s) \rightarrow T2(s)$	Change	k_{tir}
12	$RM^*(s) + RM^*(r) \rightarrow RDR(s+r)$	Combination	k_{tc}
11	$RM^*(s) + RM^*(r) \rightarrow RD(s) + RD(r)$	Disproportion	k_{td}

obtained with what we call the "simplified model" (model 3), against the predictions obtained with the "complete model" (Figures 5 and 6).

The second polymerization system addressed in this paper (Case 2) was the RAFT polymerization of styrene, at 60°C, using AIBN as initiator, and cumyl dithiobenzoate as RAFT agent. The first objective of simulating these polymerization conditions was to compare our model predictions against available experimental data (6), and to evaluate the differences among the three reaction mechanisms described in this paper ("complete", "irreversible" and "simplified") (Figures 7 and 8). The second objective was to find out if it was possible to calculate the concentration of one- and two-arm polymer radicals (adduct polymer or macroRAFT radicals) using Predici®, and to compare the calculated concentrations against those obtained with our models (Figures 9 and 10). The third and last objective sought with our simulations at the conditions of Case 2 was to evaluate the importance of the rate of production of three-arm polymer on polymerization rate and molecular weight development (Figures 11 and 12). This is an important aspect related to the retardation effect in RAFT polymerization.

Simulations at the Conditions of Case 1 using the Irreversible Model with Fortran and Predici®

The irreversible case (model 2) can be modeled with the Fortran computer program for the complete model (model 1) by making $k_{-add} = k_{-bd} = k_{-a} = k_{-b} = 0$ (see Table 1). Figure 2 shows the effects of initial initiator concentration (Figure 2a) and RAFT transfer agent

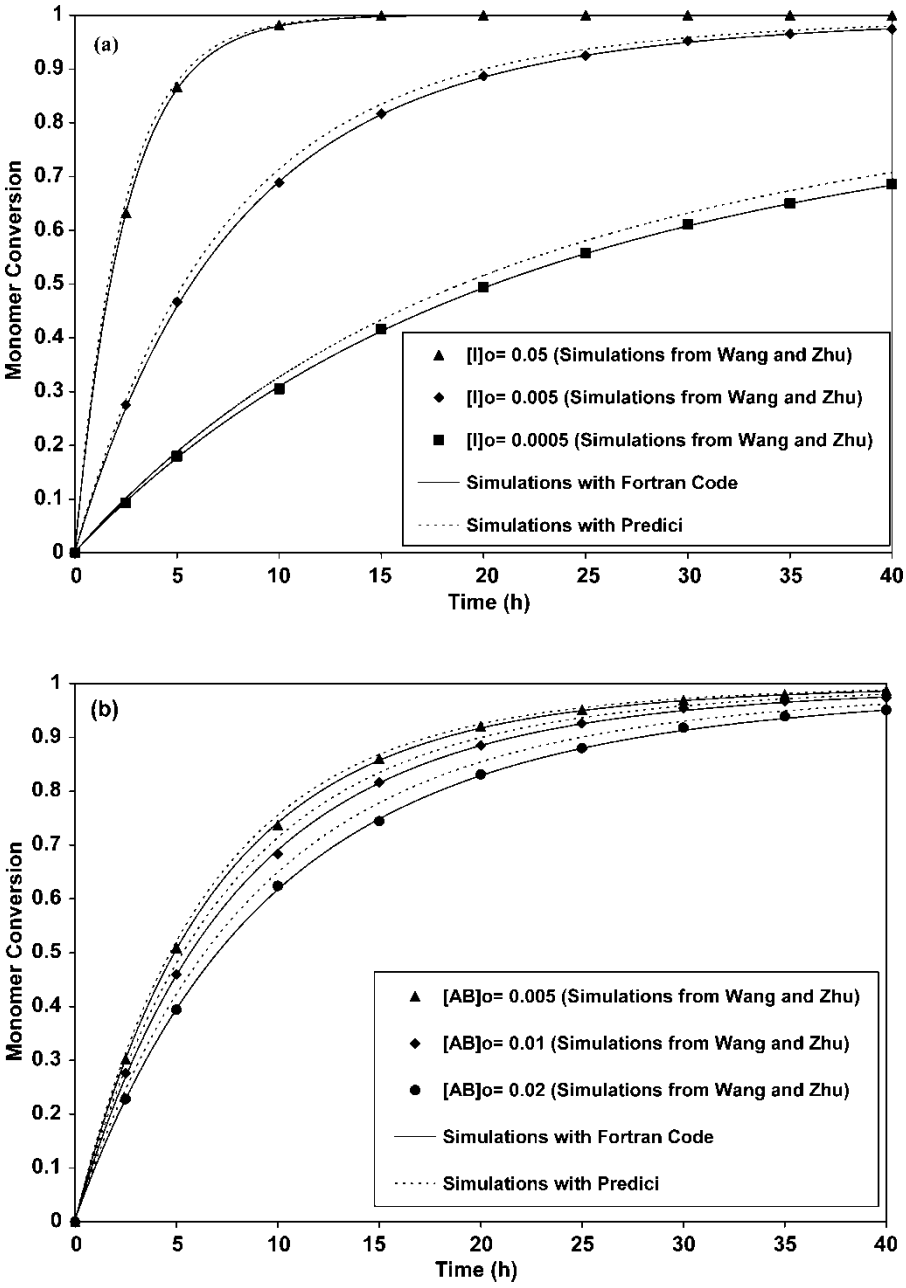

Figure 2. Effect of (a) initiator, and (b) RAFT transfer agent initial concentrations on monomer conversion in RAFT polymerization of styrene, using the "Irreversible Model" ("Model 2"). The polymerization conditions and kinetic parameters are: $[M]_0 = 5\,mol\,L^{-1}$, $[I]_0 = 5 \times 10^{-3}\,mol\,L^{-1}$ (for plot (b), variable in plot (a)), $[AB]_0 = 10^{-2}\,mol\,L^{-1}$ (for plot (a), variable in plot (b)), $k_d = 10^{-5}\,s^{-1}$, $f = 0.5$, $k_i = k_p = 10^3\,L\,mol^{-1}\,s^{-1}$, $k_{td} = k_{tc} = k_{tir} = 10^7\,L\,mol^{-1}\,s^{-1}$, $k_{add} = k_a = 10^6\,L\,mol^{-1}\,s^{-1}$, and $k_{bd} = k_b = 10^4\,s^{-1}$. All other rate constants are set equal to zero.

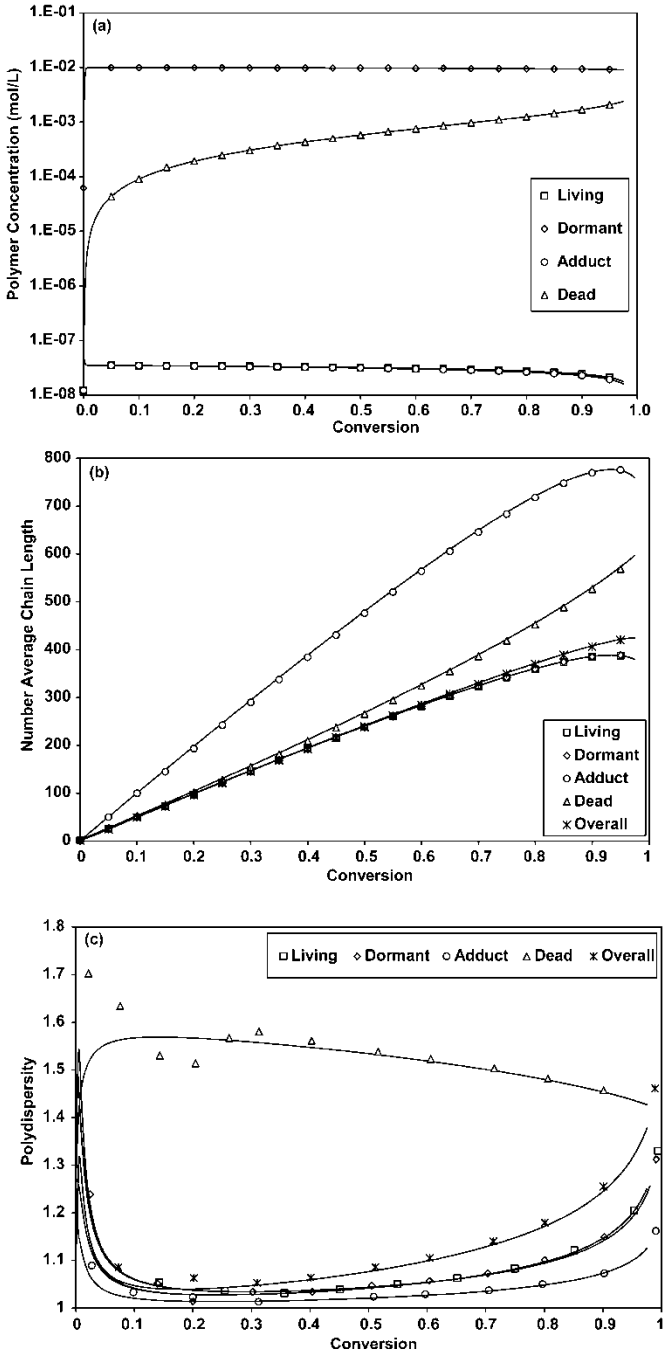

Figure 3. Development of (a) polymer concentration (zeroth moments), (b) number average chain lengths, and (c) polydispersities of the various types of polymeric species present in RAFT polymerization. The adduct symbol refers to one- and two-arm species combined. The different points represent simulations from Wang and Zhu (7) and the solid lines are calculated profiles obtained with our Fortran code, using "Model 2". In the simulations, $[I]_0 = 5 \times 10^{-3}$ mol L^{-1} and $[AB]_0 = 10^{-2}$ mol L^{-1}. Remaining polymerization conditions and kinetic parameters as in Figure 2.

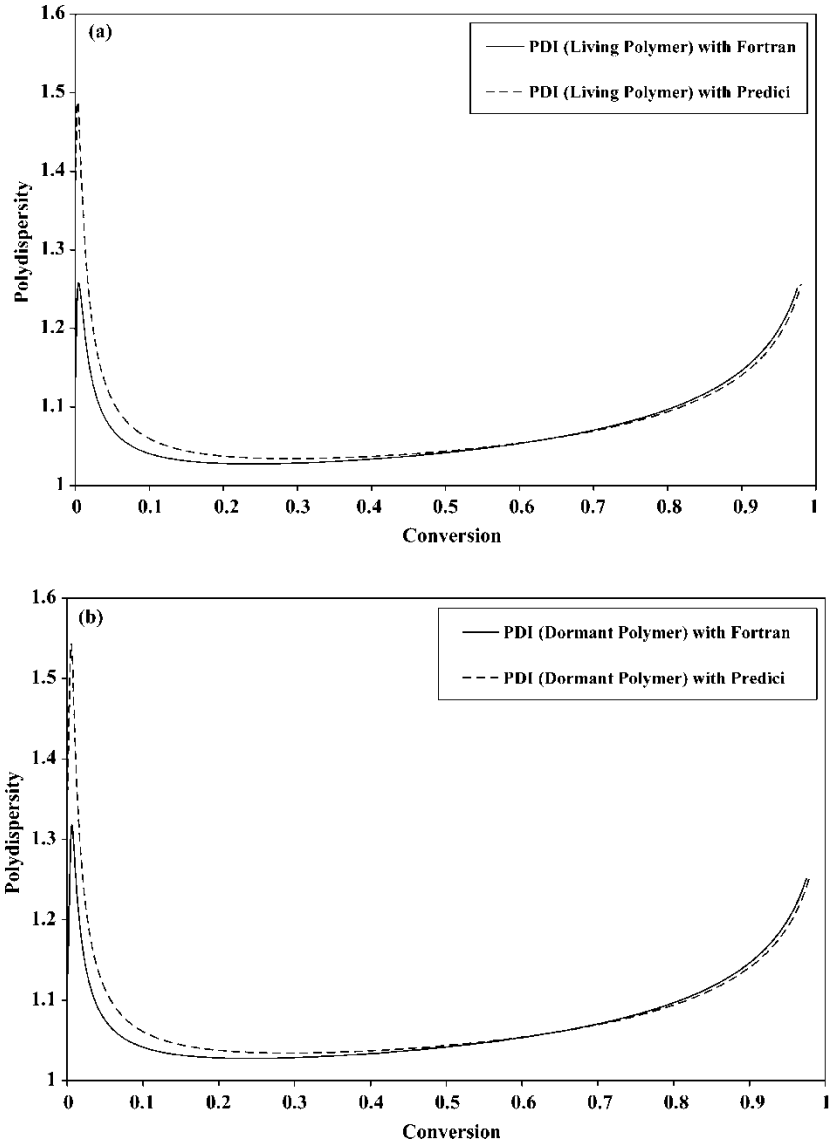

Figure 4. Comparison of calculations obtained with Fortran and Predici®, using "Model 1": PDI versus time for (a) living polymer molecules, and (b) for dormant polymer molecules. Polymerization conditions and parameters same as in Figure 3, except for the values of k_{-add}, k_{-bd}, k_{-a}, and k_{-b}, which are not equal to zero this time, but take on the following values: $k_{-add} = k_{-a} = k_b = 1 \times 10^4\ s^{-1}$, and $k_{-bd} = k_{-b} = k_a = 1 \times 10^6\ L\,mol^{-1}\,s^{-1}$.

initial concentration (Figure 2b) on polymerization rate, expressed as conversion vs. time. As expected, increasing the initial amount of initiator causes the polymerization rate to proceed faster. On the other hand, by increasing the amount of RAFT transfer agent, the polymerization rate is decreased. The profiles shown in Figure 2 seem to indicate that the effect of the amount of initiator on the polymerization rate is more pronounced than that of the amount of RAFT transfer agent. However, it should be noted that the amount of RAFT transfer agent is

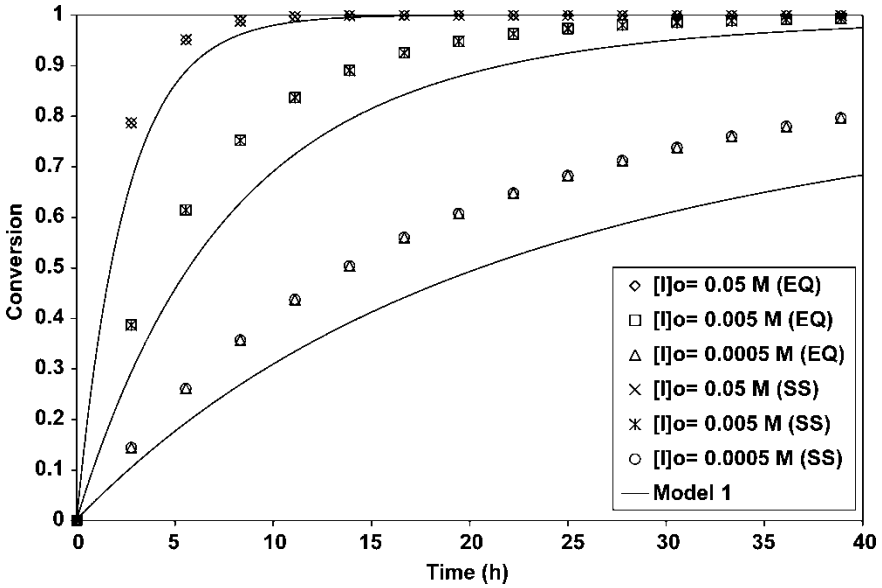

Figure 5. Comparison of performance for polymerization rate (conversion versus time) between models 1 and 3 ("Complete" and "Simplified", respectively), at the same polymerization conditions of Figure 2(a). The parameters for the complete model are as in Figure 4. For the "simplified" model see text.

being doubled or cut in half (Figure 2b), with respect to the base case, whereas the amount of initiator changes by one order of magnitude (Figure 2a). An interesting aspect to notice is that our implementation of the irreversible model coincides completely with the simulations reported by Wang and Zhu (7) (W-Z), represented by symbols in Figure 2. Although the Predici®-produced profiles of conversion versus time shown in Figure 2 lie slightly above the Fortran and W-Z ones, the agreement is very good.

Model predictions of molecular weight development for the polymerization conditions of Case 1 are shown in Figure 3. The evolution with monomer conversion of the zeroth moments (polymer concentration) of the MWDs of the different polymer species participating in the polymerization is shown in Figure 3(a). It is observed that the concentration of living species (linear polymer radicals with the radical center at the end of the chain, as well as one- and two-arm polymeric adducts) is very low, in the order of 10^{-8} mol L^{-1}, which is within the typical concentration range of conventional radical polymerization. The concentration of dead polymer is in the 10^{-4} to 10^{-3} mol L^{-1} range, which is rather low if compared with standard free-radical polymerization, but common in CLRP. The majority of the polymer is in the form of dormant polymer. Figure 3(b) shows the evolution of the number average chain length (ratio of first to zeroth moments of the MWDs) of the living, dormant, adduct (one and two-arm species grouped together), dead and overall polymer species. The CLRP typical linear behavior in the r_n versus conversion profile is clearly observed. The number average chain lengths of the living and dormant polymeric species are virtually the same, with the r_n of the dead polymer being a bit larger, and the r_n of the adduct population almost twice the value of the other populations. This is expected, since a two-arm adduct is made out of 2 polymer molecules, temporarily linked together. The average is slightly lower than twice the

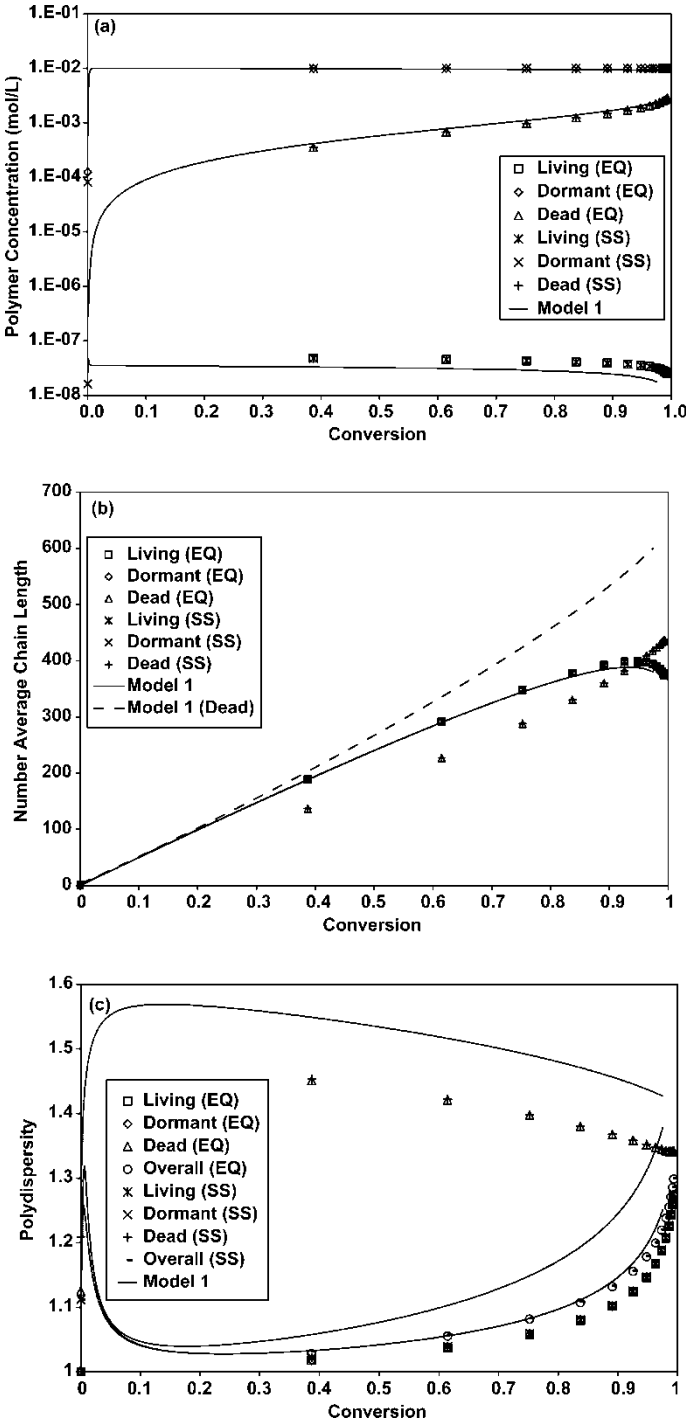

Figure 6. Comparison of performance for calculation of molecular weight development between the "Complete" and "Simplified" models: (a) polymer concentration (zeroth moment of the MWD), (b) number average chain length, and (c) polydispersity, of the different polymeric species participating in the RAFT process. Polymerization conditions and model parameters as in Figure 5.

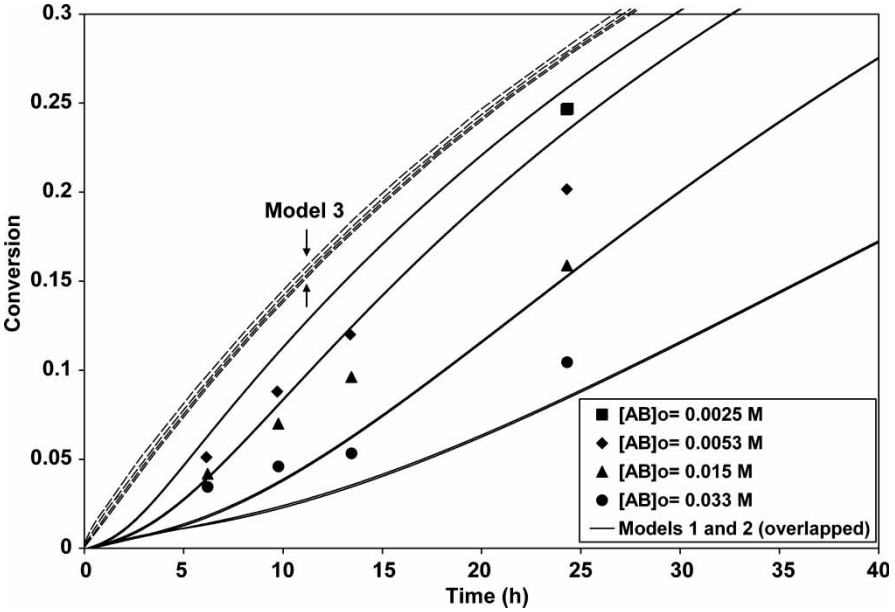

Figure 7. Comparison of model predictions obtained with models 1, 2 and 3, and experimental data (25) of conversion vs. time for the RAFT polymerization of styrene with cumyl dithiobenzoate and AIBN at 60°C. The polymerization conditions and kinetic parameters are: $[M]_0 = 5\,mol\,L^{-1}$, $[I]_0 = 3.5 \times 10^{-3}\,mol\,L^{-1}$, $k_d = 9.53 \times 10^{-6}\,s^{-1}$, $f = 0.64$, $k_i = k_p = 339\,L\,mol^{-1}\,s^{-1}$, $k_{td} = 0$, $k_{tc} = 10^7\,L\,mol^{-1}\,s^{-1}$, $k_{tir} = 0$, $k_a = k_{-b} = 5.4 \times 10^5\,L\,mol^{-1}\,s^{-1}$, $k_{add} = k_{-bd} = 3.5 \times 10^5\,L\,mol^{-1}\,s^{-1}$, and $k_b = k_{-a} = k_{bd} = k_{-add} = 3.3 \times 10^{-2}\,s^{-1}$. All other rate constants are set equal to zero.

average of the other species because of the fact that the adduct polymer shown in Figure 3 considers not only the two-arm adduct, but also the one-arm adduct polymer molecules. The PDI versus conversion profiles for these species, and the overall values are shown in Figure 3(c). The typical behavior of a CLRP system is observed. Rather large PDI values are obtained early on in the reaction, with low PDI values being obtained at the intermediate conversion range, and a small increase at high conversions. It is observed that the population of dead polymer makes the average polydispersity to increase, with respect to the PDIs of the living and dormant polymer, but given the small fraction of dead polymer present in the system, the average PDI values are still very good. Our predictions with Model 2 (Irreversible) fully coincide with the calculations obtained by Wang and Zhu (7), except for the PDI vs. conversion profile for dead polymer at low conversions, where Wang and Zhu obtained a small oscillation (see open triangles in Figure 3c), and we obtained a smooth profile. It is possible that the authors in (7) might have carried out that specific simulation with a larger tolerance in their ODE solver, hence, the numerical error was larger (which is a commonly encountered instability).

Figure 4 shows a comparison of model predictions of PDI vs. conversion, for the living and dormant populations (Figures 4a and 4b, respectively) between our Fortran program and Predici®, also at the conditions of Case 1. The only difference with the previous simulations (Figure 3) is that this time the calculations were carried out with the "complete" model (model 1), and not with the irreversible one. In this case, k_{-add}, k_{-bd}, k_{-a}, and k_{-b} are not equal to zero, but $k_{-add} = k_{-a} = k_b$ ($= 1 \times 10^4\,s^{-1}$) and $k_{-bd} = k_{-b} = k_a$ ($= 1 \times 10^6\,L\,mol^{-1}\,s^{-1}$). Everything else was the same as in the previous

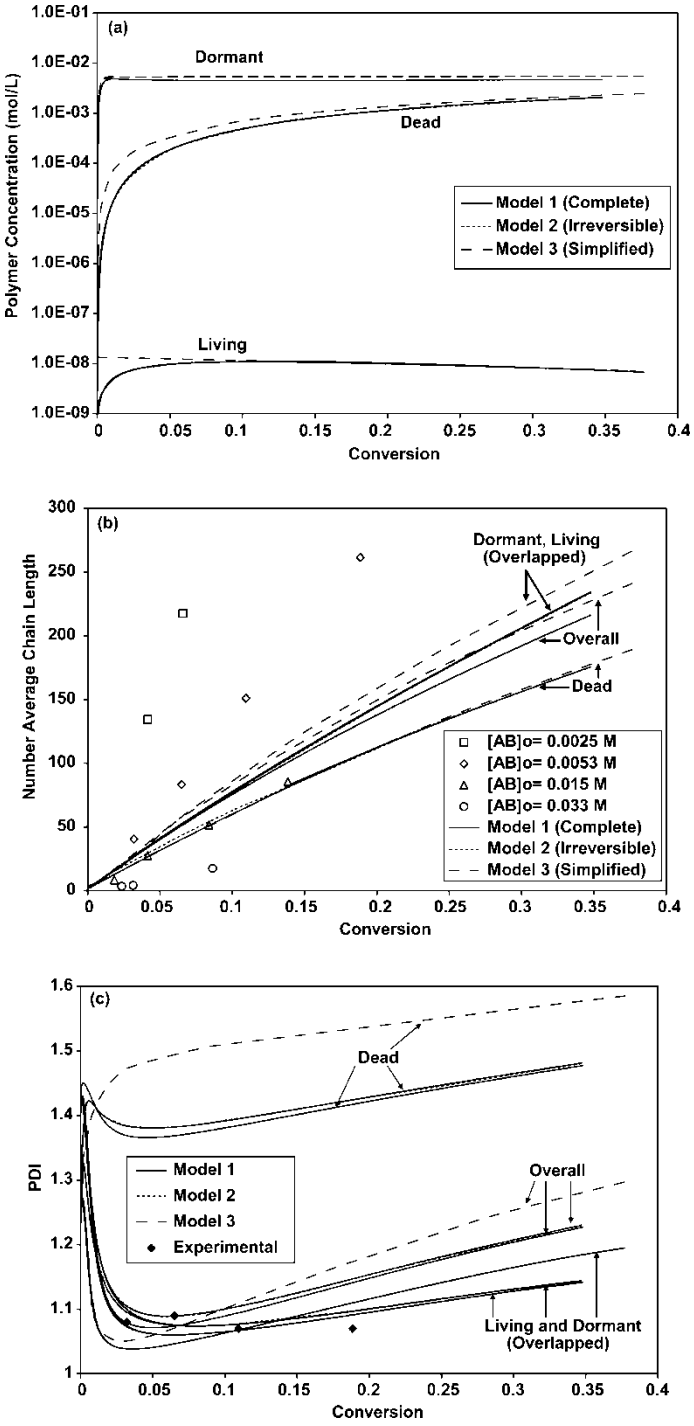

Figure 8. Comparison of model predictions obtained with models 1, 2 and 3 for (a) polymer concentration, (b) number average chain length, and (c) polydispersity of the polymeric species present in the RAFT polymerization of styrene with cumyl dithiobenzoate and AIBN at 60°C. The polymerization conditions and kinetic parameters are as in Figure 7. Experimental data in (b) and (c) are from (6).

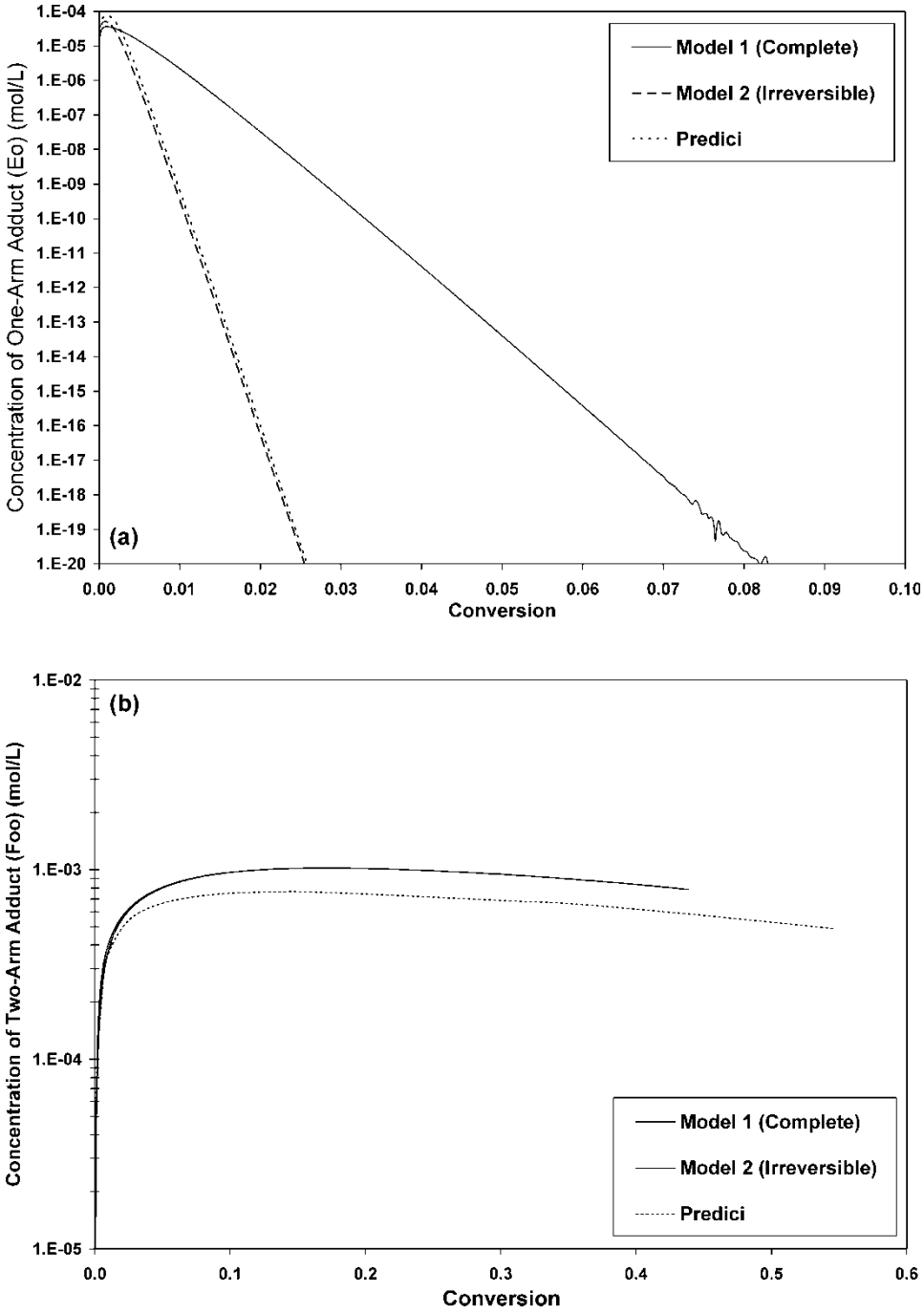

Figure 9. Comparison of model predictions for (a) concentration of one-arm adduct (E_0) vs. conversion, and (b) concentration of two-arm adduct (F_{00}) vs. conversion, obtained with the Fortran implementation of models 1 and 2, and the Predici® implementation of Model 2, for the RAFT polymerization of styrene with cumyl dithiobenzoate and AIBN at 60°C. Polymerization conditions and kinetic parameters as in Figure 7.

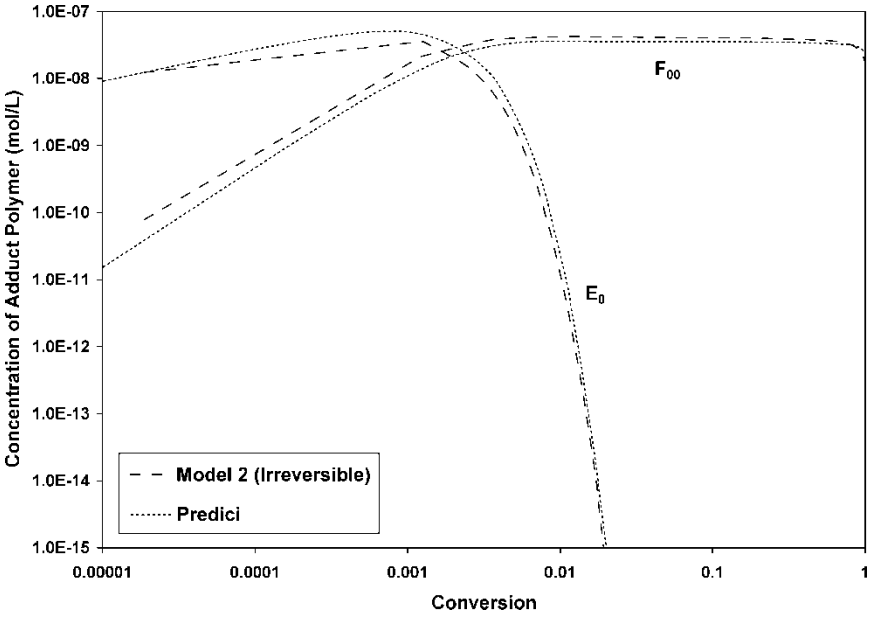

Figure 10. Evolution of the concentration profiles of one-arm (E_0) and two-arm (F_{00}) polymer adduct molecules, at the polymerization conditions and with the kinetic parameters listed in the caption of Figure 2.

simulations. It is observed that the Fortran and Predici® profiles practically overlap, with just a small overestimation of PDI obtained with Predici® at very low conversions. This overestimation of PDI obtained with Predici® at very low conversions might have been caused by the fact of using the default numerical settings of Predici® to simulate the system, whereas the Fortran simulations were carried out with very low tolerances in the ODE solver (DDASSL). If Figures 3c and 4 are carefully scrutinized, it will be noticed that the profiles for PDI versus conversion for the living and dormant species are indeed identical, regardless of the model (either 1 or 2) used to generate them.

So far, it was observed that for Case 1, Models 1 and 2 provide the same results for polymerization rate and molecular weight development. Predici® and our Fortran program provide virtually the same results. Although the Predici® profiles of Figures 3(a, b, c) are not shown, they virtually overlapped with the ones produced with our Fortran program. The aspects about the capability of Predici® to calculate the concentrations of the one-and two-arm adduct polymer species will be addresses later in this paper.

Simulations at the Conditions of Case 1 using the "Complete" and "Simplified" Models (Model 1 vs. Model 3)

As pointed out in section "Reaction Mechanism", in order to compare the predictions of the "complete" and "simplified" models, a relationship between the addition/fragmentation kinetic rate constants of the "complete" model (k_{add}, k_{-add}, k_{bd}, k_{-bd}, k_a, k_{-a}, k_b and k_{-b}, which we will call C-parameters) and the kinetic rate constants of the direct reversible

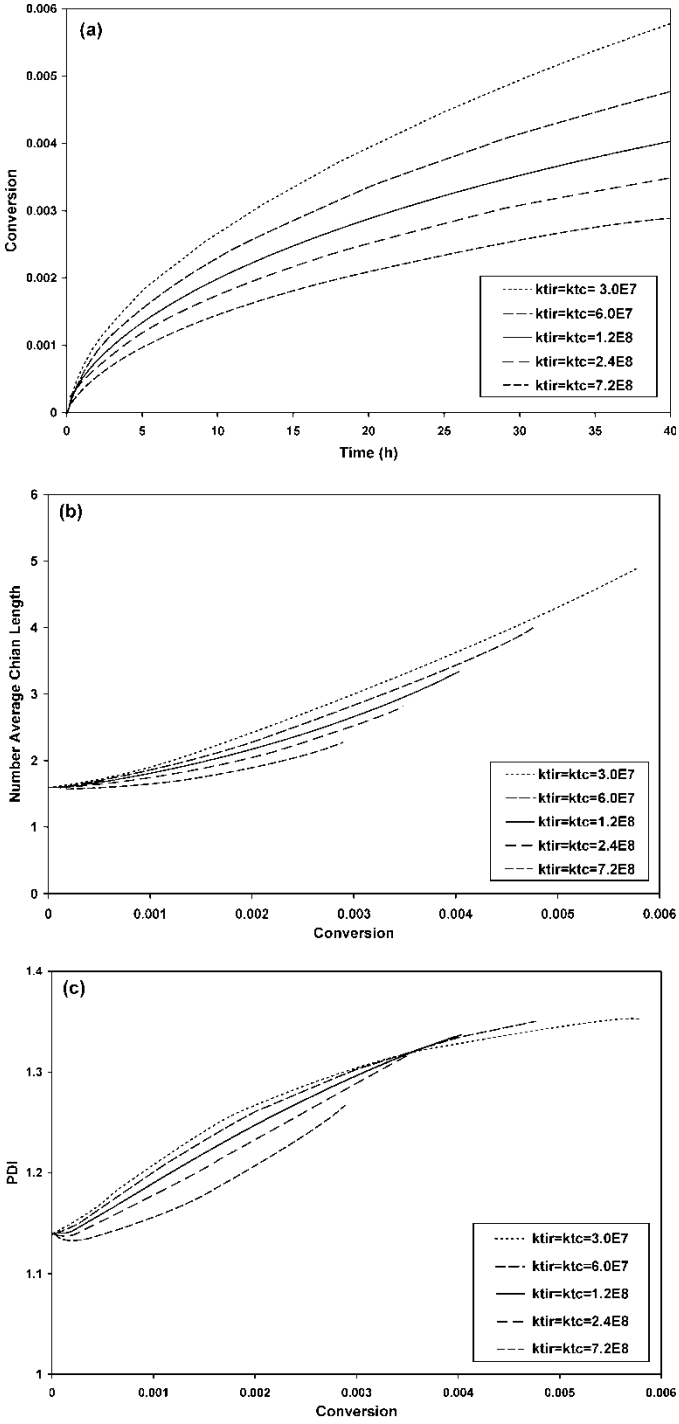

Figure 11. Effect of the kinetic rate constant for formation of three-arm polymer (k_{tir}) on (a) polymerization rate (conversion versus time), (b) number average molecular weight versus conversion, and (c) PDI versus conversion, assuming $k_{tir} = k_{tc}$. Calculations with our Fortran implementation of Model 2. Initial conditions and values of the other kinetic parameters as in Figure 7.

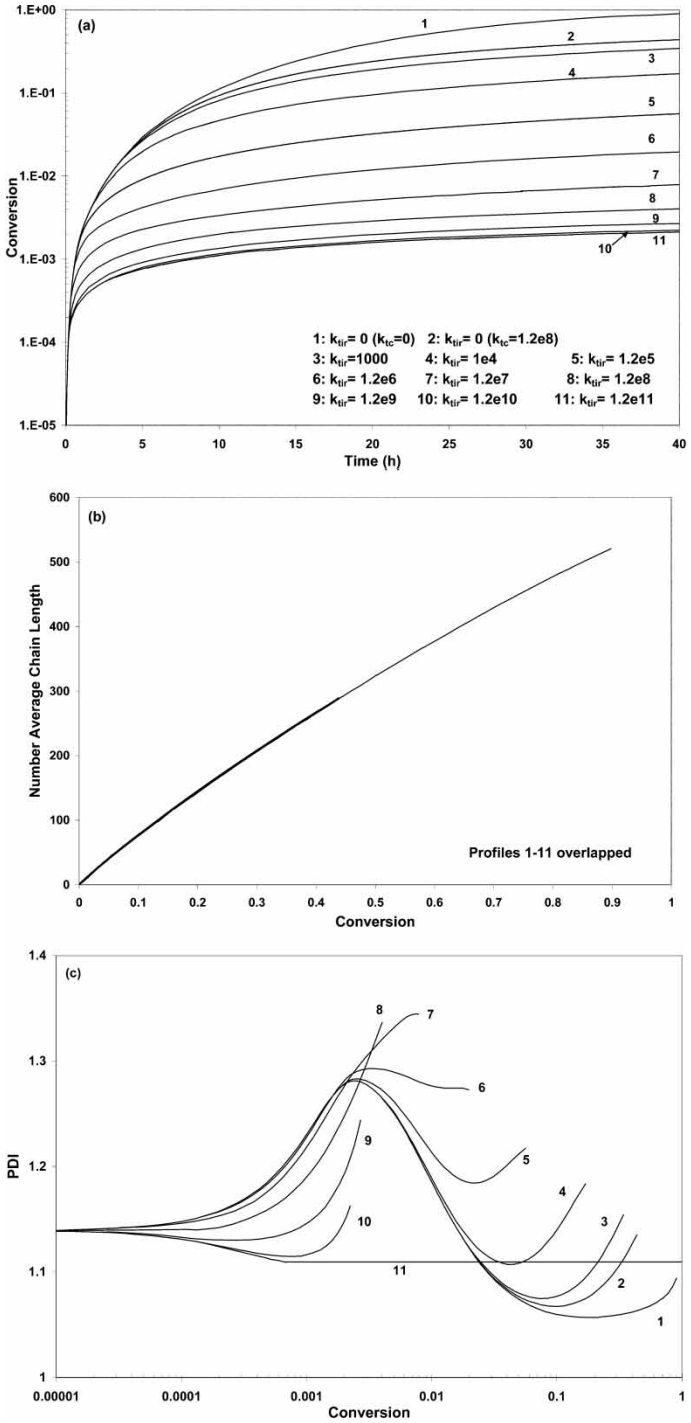

Figure 12. Effect of the kinetic rate constant for formation of three-arm polymer (k_{tir}) on (a) polymerization rate (conversion vs. time), (b) number average chain length vs. conversion, and (c) PDI vs. conversion. Calculations with our Fortran implementation of Model 2. Initial conditions and values of the other kinetic parameters as in Figure 7.

chain transfer of the "simplified" model (k_1, k_2, k_3 and k_4, which we will call S-parameters) must be established. In order to obtain such a relationship two approaches will be followed. In the first one, it will be assumed that the addition stage of the chain equilibration reaction reaches equilibrium (see #8 and 10 of Table 1). This equilibrium approach will be identified as "EQ" in the discussion and figures of this section. In the second approach, it will be assumed that the rates of production and consumption of adduct polymer are very similar in magnitude, such that a quasi-steady state assumption (QSSA) can be established. This QSSA case will be identified as "SS" in the discussion and figures of this section.

There are two pieces of information needed to obtain the desired relationship between the C-and S-parameters. One is the material balance for the dormant polymer under the simplified reaction mechanism represented by Equations (2) and (3) (the mass balance under these circumstances being given by the second to fifth terms of Equation (19), the second and third accounting for the chain transfer to the RAFT agent, and the fourth and fifth for the chain transfer to the dormant polymer), and the second is the mass balances for the one and two-arm adduct species, given by Equations (22) and (23), respectively. In the EQ approach, substitution of the equilibrium concentration of the one-arm adduct into the mass balance of dormant polymer leads to Equations (36) and (37). Substitution of the equilibrium concentration of the two-arm adduct polymer into the dormant polymer mass balance equation leads to Equations (38) and (39). In the SS approach, the steady state concentrations of the one-arm and two-arm adduct polymers are obtained by setting Equations (22) and (23) equal to zero, substituting these expressions into the dormant polymer mass balances, and comparing term by term with the dormant polymer mass balance from the simplified reaction mechanism. This SS approach leads to Equations (40) to (43). Similar relationships have been obtained by others (see, for instance, Equations (3) and (4) of reference 3).

$$k_1^{EQ} = k_{bd}\frac{k_{add}}{k_{-add}} \tag{36}$$

$$k_2^{EQ} = k_{-bd} \tag{37}$$

$$k_3^{EQ} = k_b\frac{k_a}{k_{-a}} \tag{38}$$

$$k_4^{EQ} = k_{-b} \tag{39}$$

$$k_1^{SS} = \frac{k_{bd}k_{add}}{k_{-add} + k_{bd}} \tag{40}$$

$$k_2^{SS} = k_{-bd}\left(1 - \frac{k_{bd}}{k_{-add} + k_{bd}}\right) \tag{41}$$

$$k_3^{SS} = \frac{k_b k_a}{k_{-a} + k_b} \tag{42}$$

$$k_4^{SS} = k_{-b}\left(1 - \frac{k_b}{k_{-a} + k_b}\right) \tag{43}$$

Figures 5 and 6 show predicted profiles of polymerization rate at three different initiator concentrations, and molecular weight development at the reference conditions

(the same polymerization conditions as in Figure 2b), respectively, calculated with the "simplified" model (Model 3), and compared against the calculations obtained with model 1 (solid lines). In the previous section it was found that Models 1 and 2 provide the exact same results for Case 1. In the case of polymerization rate, it is observed in Figure 5 that significant overestimation is obtained when the "simplified" model is used. As observed in Figure 6a, the concentration of dormant polymer is adequately predicted with Model 3, but the concentration of dead polymer is slightly underestimated, and the concentration of living polymer is somewhat overestimated. The agreement between Models 1 and 3 is adequate for number average chain length of dormant and living polymer, but r_n of the dead polymer is significantly underestimated (Figure 6b) with Model 3. The PDIs of living, dormant and dead polymer are all underestimated with Model 3, as observed in Figure 6c. It is also noted that with the set of kinetic constants for Model 1 used in these calculations, the results obtained with kinetic rate constants for the "simplified" model calculated from them with Equations (36) to (39) for the "equilibrium" (EQ) and (40) to (43) for the "steady-state" (SS) approaches, are identical.

Although there are some differences between the results obtained when the adduct is considered (Models 1 and 2) or suppressed (Model 3), the qualitative features of the polymerization seem to be well described with all three models, at least for the conditions of Case 1. This result would suggest that using Model 3 could be adequate to model RAFT polymerization, provided that the kinetic rate constants are adequately fine-tuned. However, before jumping to premature conclusions, the case of a more realistic polymerization situation will be addressed in the following section.

Simulation of the RAFT Polymerization of Styrene at 60°C with AIBN and Cumyl Dithiobenzoate (Case 2) using the Three Models

Figure 7 shows the effect of the concentration of cumyl dithiobenzoate (RAFT agent) on polymerization rate for the RAFT polymerization of styrene, at 60°C, using AIBN as initiator (Case 2). This polymerization system was studied experimentally and modeled using Predici® by Barner-Kowollik et al. (6). It is observed that the polymerization proceeds quite slowly in the four cases shown, not reaching a conversion higher than 25% in the case with the lowest amount of RAFT agent, after 25 h of polymerization. As expected, the higher the amount of RAFT agent, the lower the polymerization rate. Although the qualitative trend is well captured by the complete and irreversible models (models 1 and 2 which are fully overlapping in Figure 7), the agreement of our simulations with the experimental data of Barner-Kowollik et al. (6) is not as good as the agreement obtained by the authors with their Predici® calculations. Since we used the kinetic rate constants reported by them (fitted to their experimental data), and considering that in our preceding case study (Case 1) we found that the simulations obtained with models 1 and 2, and with our implementation of the complete model in Predici®, were in good agreement, this discrepancy seems surprising. Although our three models allow the chain transfer to RAFT agent reaction to proceed irreversibly, and without the formation of an intermediate adduct (reaction #7 in Table 1), which is how Barner-Kowollik et al. (6) modeled the polymerization, in our calculations we considered the reaction to be reversible, with the formation of a one-arm adduct (reaction #8 in Table 1). That difference in the reaction

mechanism, although subtle, explains the difference between our simulations and those of Barner-Kowollik (6). It is interesting to note from Figure 7 that the predictions with the "simplified" model show a very small effect of the concentration of RAFT agent, with the four profiles corresponding to different RAFT initial concentrations almost overlapping. This is a major drawback of the "simplified" model (Model 3).

Figure 8 shows the concentration profiles of living, dormant and dead polymer (Figure 8a), the evolution of the number average chain lengths of the same polymeric species (Figure 8b), and their corresponding PDIs (Figure 8c). The predicted profiles were obtained with the three models described in this paper, as a global comparison. Also shown in Figures 8b and 8c are experimental data from Barner-Kowollik et al. (6). It is observed from Figure 8a that the concentration of living polymer decreases slightly, but remains in the order of 10^{-8} mol L^{-1} in the conversion range analyzed (up to 40% monomer conversion). The concentration of dormant polymer remains fairly constant, in the order of 0.005 mol L^{-1}, and the concentration of dead polymer increases from about 10^{-7} to about 10^{-3} molar in that conversion range. That means that under these polymerization conditions the amount of dead polymer is not negligible. The predictions obtained with Models 1 and 2 completely overlap, whereas the predicted concentration profiles with the "simplified" model are higher in all three cases.

The predictions of number average chain length for the three polymeric species (living, dormant and dead) obtained with the simplified model are higher than those obtained with Models 1 and 2 for the dormant, living and overall species, but fairly close for the dead polymer (Figure 8b). It is observed that our predictions of overall r_n at $[AB]_0 = 0.0053$ mol L^{-1} are lower than the experimental data (considering here that the data are reliable). The experimental data at the other RAFT agent concentrations are included as reference, to obtain a better perspective of how large the deviation was. The simulated profiles at the other concentrations were not included in the plot. This disagreement between model predictions and experimental data may be explained once again by the fact of using reaction #8 instead of reaction #7 for the reaction of chain transfer to RAFT agent, namely, that there are some differences in the reaction mechanism used by Barner-Kowollik et al. (6) and the one used by us. Figure 8c shows the predicted profiles of PDI versus conversion for the three polymeric species, as well as the overall values, and the experimental data (6) for the overall population. The predicted profiles show logical results, with the PDI profiles of the living and dormant polymer completely overlapping at the lowest values, the PDIs of the dead polymer being higher than the others, but not more than 1.5, and the overall PDI values lying in between, closer to the PDIs of the living/dormant polymer. The agreement between Models 1 and 2 is good, with the profiles almost overlapping, but the predictions with Model 3 are significantly higher in all cases. The agreement between the profile for the overall population and the experimental data is good at low conversions (lower than 10%), whereas the experimental PDIs seem to indicate a constant behavior while the predicted profile shows a gradual increase. Since the data set is rather limited, it is not known if the predicted profile would show a maximum followed by a decrease later. However, the predicted profiles obtained for Case 1 suggest that the PDI profiles for the living, dormant and overall populations should keep increasing. It would be desirable to consider more experimental data, covering the full conversion range. However, the typical scenario so far is that most experimental studies on RAFT polymerization are restricted (if at all available) rather to the low conversion regime.

The results obtained with Case 2 suggest that although Model 3 provides good qualitative behavior, it is not reliable for quantitative purposes that involve interpolating or extrapolating beyond the region studied experimentally.

Comparison of the Predictions of Concentration of One and Two-arm Polymer Adduct between our Implementation of Models 1 or 2 and Predici®

Figure 9 shows predicted profiles of concentrations of one- (Figure 9a) and two-arm (Figure 9b) polymer adduct (E_0 and F_{00}, respectively) vs. monomer conversion, at the polymerization conditions of Case 2. It is observed that the one-arm adduct is consumed very rapidly, starting from a fairly large concentration, in the order of 10^{-5} mol L^{-1}, to an almost complete depletion. By the time 10% of the monomer is consumed, there is practically no one-arm adduct left in the system. In the case of the two-arm polymeric adduct, there is an even larger concentration (close to 0.001 mol L^{-1}) and although it decreases with time, it does so rather slowly (see Figure 9b). One interesting aspect to point out is that the Predici® simulations and the Fortran simulations with Model 2 for the case of E_0 (Figure 9a) agree very well. E_0 in Predici® was obtained directly from the concentration of variable "RMAB(s)" (see Table 3) and F_{00} was obtained from the concentration of the "memory" variable used in Predici® to account for the adduct (either D(s) or DA(s) from Table 3). The predicted profile of E_0 versus time with Model 1 decays less rapidly but still the agreement is good. In the case of F_{00}, Models 1 and 2 overlap, and the Predici profile deviates a little, but the agreement is still satisfactory. These results show two important aspects: (1) at the conditions of Case 2 the one-arm adduct is a short lived species, but the two-arm adduct is rather stable, and (2) the predictions of E_0 and F_{00} obtained with Predici® agree very well with the results obtained with the model of Wang and Zhu (7) (Model 2 of this paper). We will revisit these statements shortly.

In the simulations of molecular weight development for Case 1 (Figure 3) it was mentioned that the calculations of $E_0 + F_{00}$ (what is called "adduct" in Figure 3) obtained with Predici® agreed well with the Fortran ones, but the profiles were not shown. Those profiles are now shown in Figure 10. It is observed that the agreement between Model 2 and Predici® is very good, namely, we can calculate without any problem the concentration profiles of the adduct polymeric species using Predici®. Another interesting observation is that at the conditions of Case 1, the maximum concentration of E_0 is much lower than in case 2 and also decreases very rapidly, whereas F_{00} again decreases more slowly and its concentration is very low, an indication that these radicals are short-lived species (meaning that as soon as they are produced they are consumed).

The results obtained for case 2 (see 1 and 2 above) suggest that Barner-Kowollik et al. (14) are correct when they state that the polymer adduct is a stable species. However, the results obtained for Case 1 indicate that Wang and Zhu (7) are also correct when they state that the polymeric adduct is a short-lived species. In other words, the polymer adduct is stable when $k_b = 10^{-2}$ s^{-1} and it is a short-lived species when $k_b = 10^4$ s^{-1}. What is the true physical nature of these radical species needs to be further studied, but what is clear is that the models which consider the presence of the adduct (Models 1 and 2 of this paper, this last one being the same as the model by Wang and Zhu (7)) can capture well these possible operating regions. These results show the necessity of finding more direct ways to estimate some of the kinetic rate constants associated to complex reaction mechanisms, such as the RAFT one. Another important aspect to point out is that Wang et al. (15) are incorrect when they state that the concentrations of the polymeric adducts can not be calculated with Predici®.

Effect of Three-arm Dead Polymer (Intermediate Termination) on Polymerization Rate and Molecular Weight Development (Retardation Effect)

Figures 11 and 12 show the importance of the magnitude of the rate of formation of three-arm dead polymer (intermediate termination) from the reaction between two-arm polymeric adduct and linear polymer radical molecules, represented by the magnitude of the kinetic rate constant k_{tir}, on polymerization rate and molecular weight development of the RAFT polymerization of styrene at 60^0C using cumyl dithiobenzoate and AIBN (Case 2). In the simulations of Figure 11 it is assumed that $k_{tc} = k_{tir}$, so that both constants are varied together. In Figure 12 k_{tc} is assumed independent of k_{tir}.

It is observed in Figure 11a that if k_{tc} takes on the typical values of termination by combination in conventional free-radical polymerization (which seems adequate for CLRP), the polymerization proceeds extremely slowly. This strong retardation effect does not seem to significantly affect the number average molecular weight in the early stages of the polymerization (Figure 11b), and it seems to only affect the PDI values at extremely low conversions (Figure 11c). Although the formation of three-arm stars seems like a plausible explanation of the retardation effect, it seems from our simulations that the kinetic rate constant associated to that reaction (k_{tir}) should be much lower than k_{tc} (a chemically-controlled k_t in general).

The case of $k_{tir} \leq k_{tc}$, shown in Figure 12, seems more likely. It is observed that the polymerization rate can be easily tuned to any observed experimental data by adequately choosing the value of k_{tir} (see profiles 2 to 11 in Figure 12a), without significantly affecting the r_n vs. conversion profile, as observed in Figure 12b, and with only significant effects on PDI in the very early stages (low conversions) of the polymerization (Figure 12c). It has been established that the retardation effect is not a one factor problem, depending on the particular RAFT agent/monomer combination, and the polymerization conditions. In this section we only addressed the specific explanation based on the formation of a three-arm dead polymer molecule, put forward in references (18–21). The models proposed (or evaluated) here can also be used as a valuable tool to address these (and other) issues.

Conclusions

Three plausible variations of the reaction mechanism for RAFT polymerization were evaluated and compared at the modeling (simulation) stage, and also with a limited set of experimental data. It was found that the "irreversible" model proposed by Wang and Zhu (7) provides the same results obtained with the "complete" model. This result is strictly valid when $k_a = k_{-b}$ and $k_b = k_{-a}$ (condition used in order to compare with other studies from the literature), a very reasonable assumption for many cases. The "complete" model presented here is very general and can reduce to many special situations in the literature. Both models show good agreement with trends known for this system, and with the experimental data of Barner-Kowollik et al. (6). Finally, the third "simplified" model provides good qualitative description of the process, but the effect of the RAFT agent concentration is not captured adequately.

It was demonstrated that the literature controversy around the six order of magnitude difference in the value of k_b (14, 15) has nothing to do with inadequate modeling. It is only related to the specific values of the kinetic rate constants chosen, which can represent equally plausible, yet very different physical situations. Modeling and experimentation

complement each other, and both may be heavily influenced by the appropriate design of experiments and effective parameter estimation (especially with highly correlated parameters in kinetic models). In many situations in polymerization modeling, especially with new systems like RAFT, not only availability but also reliability of process data may accentuate the importance of the above issues (and are usually the cause of many misinterpretations). Polic et al. (26) offer some suggestions with respect to the above important (yet frequently ignored) issues.

Finally, we have shown herein that the Predici® implementation of the RAFT process is correct (in agreement with Wulkow et al. (16)), and have explicitly demonstrated this via calculations of the concentrations of one-and two-arm adduct species.

Nomenclature

[]	Denotes molar concentration, mol L^{-1}
AB	Raft agent
$B^{\bullet}$	Primary radical from fragmentation of the RAFT agent ("R" group of the RAFT molecule shown in Figure 1)
CTA	Non-RAFT chain transfer agent
$CTA^{\bullet}$	Primary free radical from chain transfer to CTA
D	Dimer molecule
$D^{\bullet}$	Dimeric free radical
E_m	m-th moment of the one-arm adduct polymer population (m = 0, 1, 2, . . .), mol L^{-1}
$F_{m,n}$	Moment of order m on one arm and n on the other of the two-arm adduct polymer population (m, n = 0, 1, 2, . . .), mol L^{-1}
$G_{a,b,c}$	Moment of order a on one arm, b on the second arm and c on the third one of the three-arm dead polymer population (a, b, c = 0, 1, 2, . . .), mol L^{-1}
I	Initiator
k_1	See definition in equation (36) (EQ superscript) or (40) (SS superscript)
k_2	See definition in equation (37) (EQ superscript) or (41) (SS superscript)
k_3	See definition in equation (38) (EQ superscript) or (42) (SS superscript)
k_4	See definition in equation (39) (EQ superscript) or (43) (SS superscript)
k_a	Kinetic rate constant for the forward addition step of the chain equilibration reaction (see reaction #10 of Table 1), L mol^{-1} s^{-1}
k_{-a}	Kinetic rate constant for the reverse fractionation step of the chain equilibration reaction (see reaction #10 of Table 1), s^{-1}
k_{add}	Kinetic rate constant for the forward addition step of the reversible chain transfer to RAFT agent reaction (see reaction #8 of Table 1), L mol^{-1} s^{-1}
k_{-add}	Kinetic rate constant for the reverse fractionation step of the reversible chain transfer to RAFT agent (see reaction #8 of Table 1), s^{-1}
k_b	Kinetic rate constant for the forward fractionation step of the chain equilibration reaction (see reaction #10 of Table 1), s^{-1}
k_{-b}	Kinetic rate constant for the reverse addition step of the chain equilibration reaction (see reaction #10 of Table 1), L mol^{-1} s^{-1}
k_{bd}	Kinetic rate constant for the forward fractionation step of the reversible chain transfer to RAFT agent (see reaction #8 of Table 1), s^{-1}

k_{-bd}	Kinetic rate constant for the reverse addition step of the reversible chain transfer to RAFT agent (see reaction #8 of Table 1), L mol^{-1} s^{-1}
k_d	Kinetic rate constant for the initiator decomposition, s^{-1}
k_{dim}	Dimerization kinetic rate constant, L mol^{-1} s^{-1}
k_{fm}	Kinetic rate constant for chain transfer to monomer, L mol^{-1} s^{-1}
k_{fS}	Kinetic rate constant for chain transfer to solvent, L mol^{-1} s^{-1}
k_{fT}	Kinetic rate constant for chain transfer to CTA, L mol^{-1} s^{-1}
k_i	Kinetic rate constant for the first propagation step, L mol^{-1} s^{-1}
k_p	Propagation kinetic rate constant, L mol^{-1} s^{-1}
k_t	Termination (overall) kinetic rate constant, L mol^{-1} s^{-1}
k_{tc}	Termination by combination kinetic rate constant, L mol^{-1} s^{-1}
k_{td}	Termination by disproportionation kinetic rate constant, L mol^{-1} s^{-1}
k_{tr}	Kinetic rate constant for irreversible chain transfer to the RAFT agent (see reaction #7 of Table 1), L mol^{-1} s^{-1}
k_{thi}	Kinetic rate constant for thermal self-initiation, L mol^{-1} s^{-1}
k_{tir}	Intermediate termination kinetic rate constant (see reaction #13 of Table 1), L mol^{-1} s^{-1}
M	Monomer
$M^{\bullet}$	Monomeric free radical
M_n	Number average molecular weight, g mol^{-1}
M_{rep}	Monomer molecular weight, g mol^{-1}
M_w	Weight average molecular weight, g mol^{-1}
PDI	Polydispersity index
Q_m	m-th moment of the polymer population produced by termination by disproportionation ($m = 0, 1, 2, \ldots$), mol L^{-1}
RD_r	Dead polymer molecule of size r from termination by disproportionation
RD_rR	Dead polymer molecule of size r from termination by combination
$R_{in}^{\bullet}$	Primary free radical from initiator decomposition
$RM_r^{\bullet}$	Polymer radical of size r
RM_rA	Dormant polymer of size r
$RM_r\mathring{A}B$	One-arm adduct of size r
$RM_r\mathring{A}RM_s$	Two-arm adduct (macroRAFT radical) of size $r + s$
r_n	Number average chain length
r_w	Weight average chain length
S	Solvent
$S^{\bullet}$	Primary free radical from chain transfer to solvent
S_m	m-th moment of the polymer population produced by termination by combination ($m = 0, 1, 2, \ldots$), mol L^{-1}
Y_m	m-th moment of the living polymer population ($m = 0, 1, 2, \ldots$), mol L^{-1}
Z_m	m-th moment of the dormant polymer population ($m = 0, 1, 2, \ldots$), mol L^{-1}

Acknowledgements

Financial support from the following sources is gratefully acknowledged: Science and Technology National Council of Mexico (CONACYT) (Project CIAM U40259-Y and graduate scholarships to J. P. -D. and G. J. -S.), CNPq (Brazil), and Natural Sciences and Engineering Research Council (NSERC, Canada), through an Inter American

Materials Collaboration (IAMC or CIAM) joint project; "Dirección General de Asuntos del Personal Académico" (DGAPA) (PASPA Program) of UNAM and the Department of Chemical Engineering of the University of Waterloo (UW) (for funding of E.V. -L.'s research stay at UW).

References

1. Matyjaszewski, K. (2003) Controlled/Living Radical Polymerization: State of the Art in 2002. In *Advances in Controlled/Living Radical Polymerization*; Matyjaszewski, K. (ed.), American Chemical Society: Washington, D.C., ACS Symposium Series 854, 2–9.
2. Moad, G., Mayadunne, R.T.A., Rizzardo, E., Skidmore, M., and Thang, S.H. (2003) Kinetics and Mechanism of RAFT Polymerization. In *Advances in Controlled/Living Radical Polymerization*; Matyjaszewski, K. (ed.), American Chemical Society: Washington, D.C. ACS Symposium Series 854, 520–535.
3. Moad, G., Rizzardo, E., and Thang, S.H. (2005) *Aust. J. Chem.*, 58: 379–410.
4. Li, L., He, J.P., and Yang, Y.L. (2000) *Chem. J. Chinese Univ.*, 21: 1146–1148.
5. Zhang, M. and Ray, W.H. (2001) *Ind. Eng. Chem. Res.*, 40: 4336–4352.
6. Barner-Kowollik, C., Quinn, J.F., Morsley, D.R., and Davis, T.P. (2001) *J. Polym. Sci., A: Polym. Chem.*, 39: 1353–1365.
7. Wang, A.R. and Zhu, S. (2003) *J. Polym. Sci., A: Polym. Chem.*, 41: 1553–1566.
8. Wang, A.R. and Zhu, S. (2003) *Macromol. Theory Simul.*, 12: 196–208.
9. Luo, Y.W. (2003) *Chem. J. Chinese U.*, 24 (10): 1926–1928.
10. Drache, M., Schmidt-Naake, G., Buback, M., and Vana, P. (2005) *Polymer*, 46: 8483–8493.
11. Theis, A., Feldermann, A., Charton, N., Davis, T.P., Stenzel, M.H., and Barner-Kowollik, C. (2005) *Polymer*, 46: 6797–6809.
12. Monteiro, M.J. (2005) *J. Polym. Sci., A: Polym. Chem.*, 43: 5643–5651.
13. Peklak, A.D.; Butté, A.; Storti, G.; Morbidelli, M. (2006) *J. Polym. Sci., A: Polym. Chem.*, 44: 1071–1085.
14. Barner-Kowollik, C., Coote, M.L., Davis, T.P., Radom, L., and Vana, P. (2003) *J. Polym. Sci., A: Polym. Chem.*, 41: 2828–2832.
15. Wang, A.R., Zhu, S., Kwak, Y., Goto, A., Fukuda, T., and Monteiro, M.S. (2003) *J. Polym. Sci., A: Polym. Chem.*, 41: 2833–2839.
16. Wulkow, M., Busch, M., Davis, T.P., and Barner-Kowollik, C. (2004) *J. Polym. Sci., A: Polym. Chem.*, 42: 1441–1448.
17. Hawthorne, D.G., Moad, G., Rizzardo, E., and Thang, S.H. (1999) *Macromolecules*, 32: 5457–5459.
18. Monteiro, M.J. and de, Brouwer H. (2001) *Macromolecules*, 34: 349–352.
19. Monteiro, M.J., Subramaniam, N., Taylor, J.R., Pham, B.T.T., Tonge, M.P., and Gilbert, R.G. (2001) *Polymer*, 42: 2403.
20. Goto, A., Sato, K., Tsujii, Y., Fukuda, T., Moad, G., Rizzardo, E., and Thang, S.H. (2001) *Macromolecules*, 34: 402.
21. Kwak, Y., Goto, A., Tsujii, Y., Murata, Y., Komatsu, K., and and Fukuda, T. (2002) *Macromolecules*, 35: 3026.
22. Greszta, D. and Matyjaszewski, K. (1996) *Macromolecules*, 29 (24): 7661–7670.
23. Bonilla, J., Saldívar, E., Flores-Tlacuahuac, A., Vivaldo-Lima, E., Pfaendner, R., and Tiscareño-Lechuga, F. (2002) *Polym. React. Eng.*, 10 (4): 227–263.
24. Uzulina, I., Kanagasabapathy, S., and Claverie, J. (2000) *Macromol. Symp.*, 150: 33–38.
25. Breman, K.E., Campbell, S.L., and Petzold, L.R. (1989) *Numerical Solution of Initial-Value Problems in Differential-Algebraic Equations*; Elsevier Science Publishing Company: New York.
26. Polic, A.L., Lona, L.M.F., Duever, T.A., and Penlidis, A. (2004) *Macromol. Theory Simul.*, 13: 115–132.